J Fluoresc (2011) 21:1249–1254
DOI 10.1007/s10895-010-0806-y

ORIGINAL PAPER

A New Strategy to Identify and Eliminate the Inner Filter Effects by Outer Filter Technique

Wansong Zong · Rutao Liu · Feng Sun · Yue Teng · Xiaoyan Fang · Jun Chai

Received: 8 March 2010 / Accepted: 29 December 2010 / Published online: 20 January 2011

Abstract To identify and eliminate the inner filter effects (IFEs), prepositive and side cells containing absorbents are fixed beside the fluorescer contained cell. In this way, excitation and emission lights can be quenched by primary and secondary outer filter effects respectively, depending on absorbent concentration and cell length. Herein the quenching of emission fluorescence caused by IFEs can be equally reduced by outer filter effects (OFEs) and the interference of IFEs was eliminated. This approach was experimentally used for identifying the interaction mode and mechanism between BSA and nanoAg. Results showed that the quenching of BSA fluorescence and synchronous fluorescence mainly attributes to IFEs, instead of static/dynamic fluorescent quenching. In view of the above, the elimination of the interference of IFEs by the design of OFEs plays an important part in the precise application of fluorescence detector.

Keywords Fluorescence quench · Inner filter effects · Correction method · Outer filter effects

Wansong Zong and Rutao Liu made equal contributions to this work and share the first authorship.

Electronic supplementary material The online version of this article (doi:10.1007/s10895-010-0806-y) contains supplementary material, which is available to authorized users.

W. Zong · R. Liu (✉) · F. Sun · Y. Teng · X. Fang · J. Chai
School of Environmental Science and Engineering, Shandong University,
27# Shanda South Road,
Jinan 250100, People's Republic of China
e-mail: rutaoliu@sdu.edu.cn

Introduction

Fluorescence-based strategies can be employed to analyze the interaction (kinetic parameters and mechanisms) between analytes, depending on whether any analyte is a fluorescer [1–4]. However, if analytes have strong absorptions, the interference of the inner filter effects (IFEs) cannot be ignored and eliminated [5–8]. Different from static/dynamic fluorescent quenching, the IFEs can quench the fluorescence signals by absorbing either the excitation light (primary IFE) or the emission light (secondary IFE) of the fluorescer [5, 6]. So it is not desirable to confuse the IFEs with static/dynamic fluorescent quenching.

Though IFEs have shown a few advantages in detecting chemicals with characteristic absorption [8–11], in most cases, they just bring in more useless interferences [5, 6, 8]. Some studies have been performed to correct the observed quenching data for IFEs by means of the mathematical corrections developed from optics phenomena and empirical equations [5, 12–14]. However, these methods are lack of flexibility in dealing with complex systems and have complex procedures, and unavailable parameters. IFEs correction based on geometric parameters in typical instruments was also performed to simplify empirical equations and improve the accuracy of corresponding results [6, 15, 16], but the determination of geometric parameters makes IFEs correction be more complex. Though mirror coating cells and special instruments (simultaneously measured absorbance and fluorescence) show good results [5, 17, 18], there are still many constraints for their widest application. Therefore, the correction of IFEs is in need of simple and efficient ways.

The aim of this thesis is to develop analogous techniques suitable for the correction of IFEs in a conventional fluorescence cell (Fig. 1a). To implement either version of

IFEs, two more cells containing absorbent are fixed in the light path and the original cell just contains fluorescer (see Fig. 1b). In this case, the excitation and/or emission lights can also be absorbed by absorbent. We define these phenomenons as the outer filter effects (OFEs), in which the primary OFE refers to the absorption of excitation light and the secondary OFE refers to the absorption of emission light. By altering absorbent concentrations in the front and side cells, the excitation light and emission light can be equally reduced by OFEs as that caused by IFEs. This strategy is experimentally applied to analyze the interactions between nanoAg and bovine serum albumin (BSA) and eliminate the IFEs of nanoAg to BSA.

Theory

The theory of identify and eliminate IFEs is well established. To quantitatively interpret our theory, we derive equations suitable for the conventional cell and the combined cells. The light intensity at the λ of excitation is I_0 and uniformly distributed, and no scattering of the excitation light is also assumed.

Correction of the Primary IFE by Primary OFE

When fluorescer and absorbent are added into the conventional fluorescence cell, according to Beer-Lambert's law [5, 8], the excitation light intensity in the cross section of exciting light is uniformly distributed and the integral intensity is

$$I_x = I_0\, e^{-\varepsilon_f c_f x} e^{-\varepsilon_a c_a x} \tag{1}$$

where subscripts f and a stand for fluorescer and absorbent, respectively. ε is the specific molar absorptivity at the λ of excitation, c is the concentration, and x is the distance between the cross section and the incident surface (see Fig. 1a). The generated fluorescence intensity is proportional to the light absorbed by the fluorescer [5, 8]:

$$F_x = \varphi_f I_x (1 - e^{-\varepsilon_f c_f d_x}) \tag{2}$$

where subscript φ stands for the fluorescence quantum efficiency, and d_x is the width of the cross section. Therefore, from Eqs. 1 and 2

$$\begin{aligned} F_x &= \varphi_f I_x (1 - e^{-\varepsilon_f c_f d_x}) = \varphi_f I_0 e^{-\varepsilon_f c_f x} e^{-\varepsilon_a c_a x} (1 - e^{-\varepsilon_f c_f d_x}) \\ &= \varphi_f I_0 (1 - e^{-\varepsilon_f c_f d_x}) e^{-\varepsilon_f c_f x} e^{-\varepsilon_a c_a x} \\ &= F_0 e^{-\varepsilon_f c_f x} e^{-\varepsilon_a c_a x} \end{aligned} \tag{3}$$

When absorbent and fluorescer are separately added into combined cells (Fig. 1b), the excitation light intensity and fluorescence intensity of each cross section are also uniformly distributed but decreased by primary OFE based on the following formulas:

$$I_x' = I_0 e^{-\varepsilon_f c_f x} e^{-\varepsilon_a c_a' M} \tag{4}$$

$$F_x' = F_0 e^{-\varepsilon_f c_f x} e^{-\varepsilon_a c_a' M} \tag{5}$$

where subscript M stands for the length of the prepositive cell.

By altering the concentration of absorbent and the length of the prepositive cell, the integral fluorescence intensity can be absorbed in the same degree as conventional mode. It is inconvenient to alter cell length and thus the adjustment of absorbent concentration is more suitable. When M=1/2L, $c_a = c_a'$, the fluorescence intensities of the middle sections are equal (Fig. 2a) and the absorbents in both modes have the same spatial effects (see supporting information). Even so, the difference between the primary IFE and primary OFE ($S_A \neq S_B$, $S_A = S_0 + S_1$, $S_B = S_0 + S_2$) must be consid-

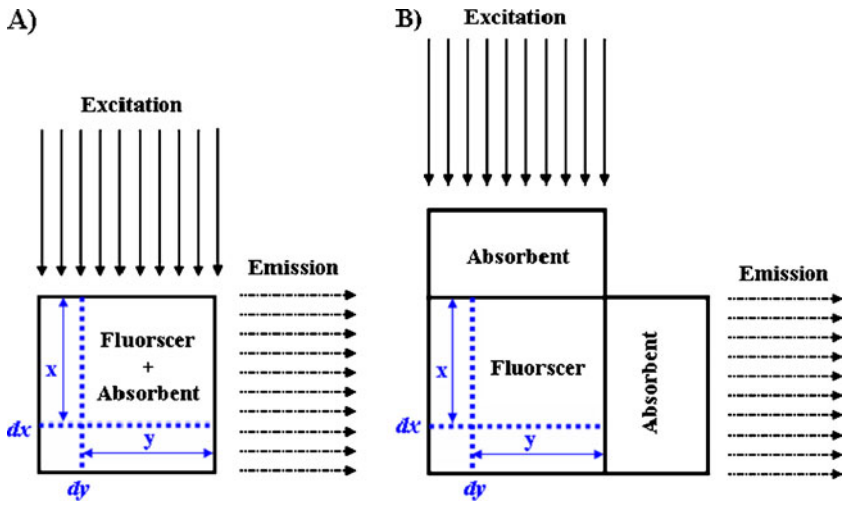

Fig. 1 IFEs in conventional fluorescence cell (**a**) and OFEs in combined cells (**b**), shown in two dimensions with cell height ignored

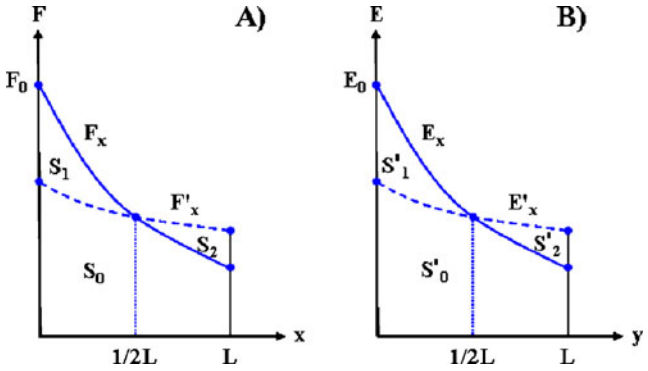

Fig. 2 **a** Influence of IFEs and OFEs on the generated fluorescence intensities (**a**) and detected fluorescence intensities (**b**) in conventional fluorescence cell and combined cells. Conditions: M=1/2L; N=1/2L; $c_a = c'_a$

ered. When S_1 and S_2 are treated as triangles while S_0 is treated as trapezium, error for primary IFE correction can be expressed as:

$$\frac{S_B - S_A}{S_B} = \frac{S_2 - S_1}{S_B} = \frac{\frac{1}{4}LF_0\left(1 - e^{-\frac{1}{2}\varepsilon_f c_f L}\right) - \frac{1}{4}LF_0 e^{-\varepsilon_f c_f L} e^{-\frac{1}{2}\varepsilon_a c_a L}\left(1 - e^{-\frac{1}{2}\varepsilon_a c_a L}\right)}{\frac{1}{2}L\left(F_0 e^{-\frac{1}{2}\varepsilon_a c_a L} + F_0 e^{-\varepsilon_f c_f L} e^{-\frac{1}{2}\varepsilon_a c_a L}\right)} \quad (6)$$

In most cases fluorescer has lower concentration and thus less absorption to excitation light intensity, so $F_0 e^{-\varepsilon_f c_f L}$ is approximately equals to F_0.

Equation 6 can be simplified into

$$\frac{S_B - S_A}{S_B} = \frac{\left(1 - e^{-\frac{1}{2}\varepsilon_a c_a L}\right)^2}{4e^{-\frac{1}{2}\varepsilon_a c_a L}} \quad (7)$$

The error depends largely on $e^{-\frac{1}{2}\varepsilon_a c_a L}$ and the correlation between them is list in Table 1A. Lower primary OFE means a minor error and higher primary OFE results in a major error. And in case the influence of primary IFE dose not exceed 30%, the error between primary IFE and primary OFE can be ignored.

Correction of the Secondary IFE by Secondary OFE

Secondary IFE does not affect the emission process [5, 6]. However, before reaching to the detector, the fluorescence signal is weakened by secondary IFE to varying degrees. In conventional mode, the fluorescence intensity in every cross section paralleling with the detector has identical distribution and just relates to x. The integral fluorescence intensity of each cross-section is:

$$F_y = \int_0^L H\frac{F_x}{HL}dx = \int_0^L \frac{F_x}{L}dx \quad (8)$$

The fluorescence intensities in the same cross-section are decreased to the same extent by fluorescer and absorbent, so F_y is used to evaluate secondary IFE. The detected fluorescence intensity of the cross section is in accordance with the following formula:

$$E_y = \kappa F_y e^{-\varepsilon'_f c_f y} e^{-\varepsilon'_a c_a y} \quad (9)$$

where subscript κ stands for the fluorescence conversion factor, ε' is the specific molar absorptivity at the λ of emission.

In correction mode, the fluorescence intensity in every cross section that parallel with the detector also has identical distribution and be weaken by primary OFE.

$$F'_y = \int_0^L H\frac{F'_x}{HL}dx = \int_0^L \frac{F'_x}{L}dx \quad (10)$$

$$E'_y = \kappa F'_y e^{-\varepsilon'_f c_f y} e^{-\varepsilon'_a c''_a N} \quad (11)$$

where subscript N stands for the length of cell.

In both mode, the integral fluorescence intensities in the conventional right angle cells are equal ($F_y L = \int_0^L F_y dy = \int_0^L F'_y dy = F'_y L$), thus $F_y = F'_y$. When N=1/2L, $c_a = c'_a$, absorbents in both modes also have identical spatial effects (see supporting information) and the fluorescence intensities from the middle sections are equal (see Fig. 2b). However, there is a difference between the secondary IFEs of both modes ($S'_A \neq S'_B$, $S'_A = S'_0 + S'_1$, $S'_B = S'_0 + S'_2$). By approximation as that performed on primary IFE/OFE, error for secondary IFE correction can be expressed as:

$$\cdot\frac{S'_B - S'_A}{S'_B} = \frac{\left(1 - e^{-\frac{1}{2}\varepsilon'_a c_a L}\right)^2}{4e^{-\frac{1}{2}\varepsilon'_a c_a L}} \quad (12)$$

The error depends on $e^{-\frac{1}{2}\varepsilon'_a c_a L}$. Lower secondary IFE means a minor error and higher secondary IFE means a major error (see Table 1B). When the influence of secondary IFE is lower than 30%, the differences between secondary IFE and secondary OFE can also be ignored.

Materials and Methods

Experimental Reagents

Bovine serum albumin (BSA, electrophoretic pure) purchased from Sinopharm Chemical Reagent Co., Ltd. was dissolved in ultrapure water to form a 1.0×10^{-5} mol L^{-1} solution and preserved at 0–4 °C. Analytical reagents Sodium citrate and silver nitrate were purchased from Sinopharm Chemical Reagent Co., Ltd.

Table 1 Errors for primary IFE (A) and secondary IFE (B) correction by primary and secondary OFEs. Conditions: M=1/2L; N=1/2L; $c_a = c'_a$

A						
Errors for primary IFE correction (M=1/2L, $c_a = c'_a$)						
Degrees of primary IFE	5%	10%	20%	30%	40%	50%
$e^{-\frac{1}{2}\varepsilon_a c_a L}$	0.95	0.90	0.80	0.70	0.60	0.50
Error	0.01%	0.28%	1.25%	3.21%	6.66%	12.5%
B						
Errors for secondary IFE correction (N=1/2L, $c_a = c'_a$)						
Degrees of primary IFE	5%	10%	20%	30%	40%	50%
$e^{-\frac{1}{2}\varepsilon'_a c_a L}$	0.95	0.90	0.80	0.70	0.60	0.50
Error	0.01%	0.28%	1.25%	3.21%	6.66%	12.5%

Experimental Apparatus

KQ-100E ultrasonic cleaner (Kunshan, Jiangsu, China), electric-heated thermostatic water bath (Jintan, Jiangsu, China) and electric blender (Xiaoyang, Jiangsu, China) were used for sample preparation. Sample analysis was performed with an FL-4600 fluorescence spectrophotometer (Hitachi, Japan) and a UV-2450 spectrophotometer (Shimadzu, Japan).

Experimental Procedures

NanoAg with a mean particle size of 40–50 nm was prepared by chemical reduction method using sodium citrate as reductant and preserved at 0–4 °C in the dark. For further prepared details, please see references [19, 20]. To evaluate the influence of IFEs on the interaction between nanoAg and BSA, the reduction of BSA fluorescence and synchronous fluorescence by nanoAg in traditional mode (single right angle cell) and in the proposed mode (combined cells) was measured.

Results and Discussion

Fluorescence and Absorption Spectra of BSA and NanoAg

The fluorescence emission spectra (at λ_{ex}=275.0 nm) of BSA, nanoAg and BSA-nanoAg are obtained in Fig. 3. It can be seen that BSA has a typical fluorescence peak at 338.0 nm while nanoAg has no fluorescence. The signal of BSA fluorescence is mainly from its intrinsic fluorophore: tryptophan and tyrosine residues [21–23]. By analyzing the variation of this peak, we can obtain information about the interactions between BSA and nanoAg. When nanoAg is added, the fluorescence intensity of BSA is quenched to certain extent but there was no significant λ_{em} shift.

To understand the quenching mechanism of BSA in depth, the influence of IFEs brought by nanoAg should be determined firstly. Ignoring IFEs and directly ascribing the relevant mechanism to static/dynamic fluorescent quenching is obviously not desirable. From the absorption spectra of nanoAg and BSA (Fig. 4), we find BSA has a characteristic absorption peak around 278.0 nm while nanoAg has one peak around 445.0 nm. Studies have

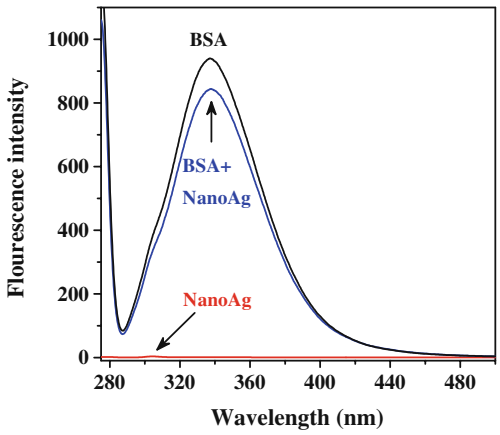

Fig. 3 The fluorescence emission spectra of BSA with and without nanoAg. Conditions: BSA 1.0×10^{-6} mol L^{-1}; NanoAg 2.0×10^{-6} g L^{-1}; excitation wavelength 275.0 nm; scan range 285.0–550.0 nm; slit width 5.0 nm; scan rate 300.0 nm/min; temperature 25 °C

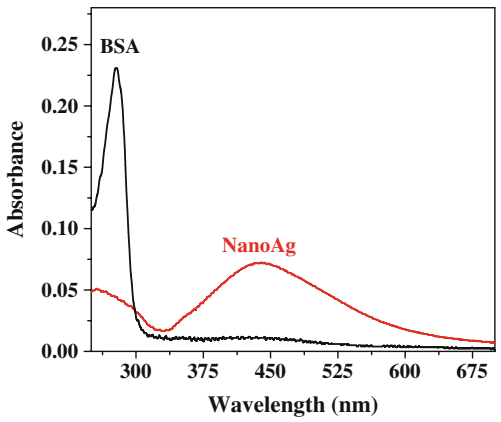

Fig. 4 The UV–visible absorption spectra of BSA and NanoAg. Conditions: BSA 5.0×10^{-6} mol L^{-1}; NanoAg 1.0×10^{-6} g L^{-1}; scan range 200.0–700.0 nm; scan speed 200.0 nm/s; sampling interval 0.2 s; temperature 25 °C

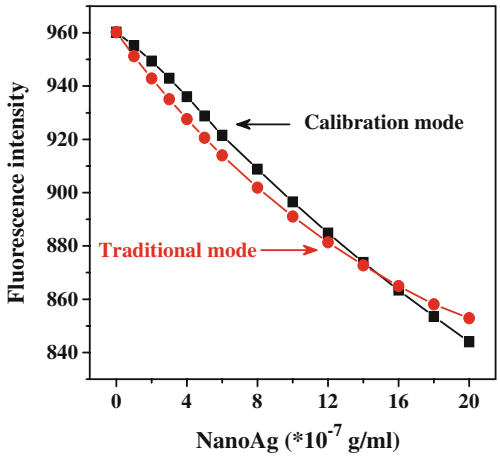

Fig. 5 Influence of NanoAg dose on the fluorescence spectra of BSA in traditional and calibration modes. Conditions: BSA 1.0×10^{-6} mol L^{-1}; excitation wavelength 275.0 nm; emission wavelength 338.0 nm; slit width 5.0 nm; temperature 25 °C

confirmed that the characteristic peak for BSA is corresponding to the aromatic ring amino acids and the absorption peak of nanoAg originates from its colloidal state [24, 25]. Comparing the absorption and fluorescence emission spectra of BSA and nanoAg, we also find the absorption spectrum of nanoAg show partial overlap with the absorption and fluorescence spectra of BSA. Thus both excitation light and the excitation-induced emission light from BSA can be absorbed by nanoAg, and it is difficult to ignore the IFEs brought by nanoAg.

Influence of NanoAg on the Fluorescence Spectra of BSA in Traditional Mode and Calibration Mode

Figure 5 shows the influence of nanoAg on the fluorescence spectra of BSA in traditional mode and calibration mode using an excitation wavelength at 275.0 nm. In traditional mode, the emission intensity of BSA reduces successively with the increase of nanoAg and fluorescence quenching happens to BSA. Due to the interfering of nanoAg, it needs to eliminate the influence of IFEs before analyzing the quenching mechanism of BSA fluorescence. In calibration mode, the emission intensity of BSA also reduces gradually with the increased nanoAg (the IFEs brought by nanoAg are directly verified). Comparing these results, we find there is a smaller difference between signals of the two modes at the same nanoAg concentrations and both curves have consistent trends. Consequently, IFEs play a leading role in the quenching of BSA fluorescence in the studied concentration range of nanoAg.

Influence of NanoAg on the Synchronous Fluorescence of BSA in Traditional Mode and Calibration Mode

The fluorescence characteristic of BSA depends primarily on its tryptophan and tyrosine residues and can be analyzed by synchronous fluorescence spectroscopy [21, 22]. Therefore, evaluating the influence of nanoAg dose on the

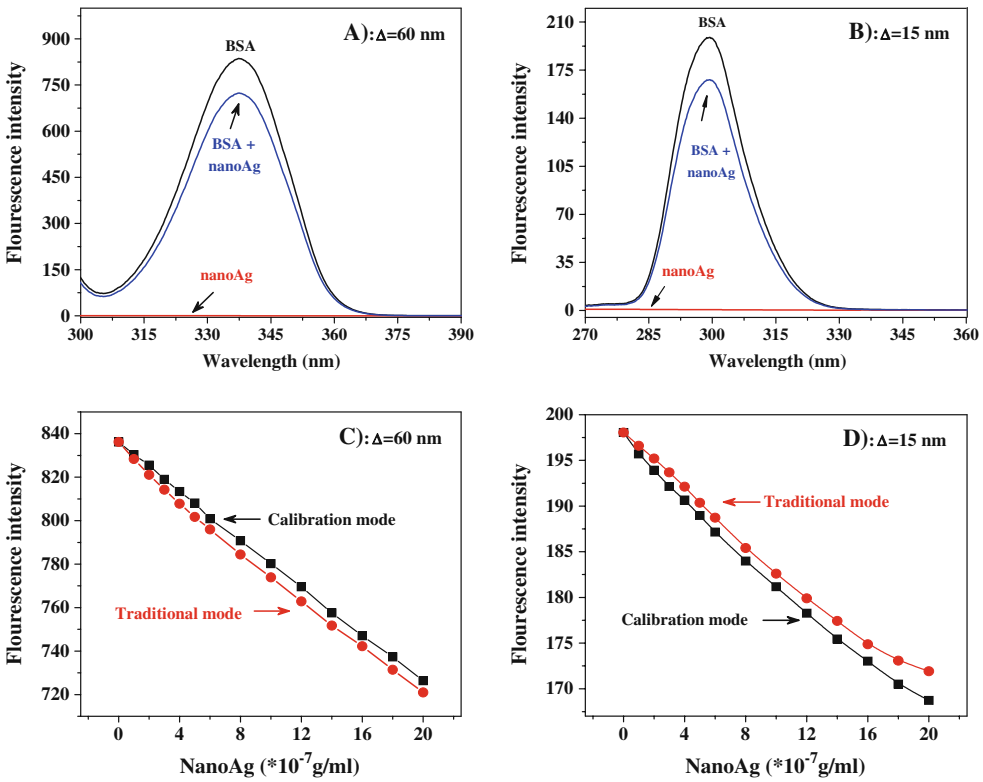

Fig. 6 The synchronous fluorescence spectra (**a**: Δ=60 nm; **b**: Δ=15 nm) of BSA with and without NanoAg, and the influence of NanoAg dose on the synchronous fluorescence spectra (**c**: Δ=60 nm, at 338.0 nm; **d**: Δ=15 nm, at 229.0 nm) of BSA in traditional and calibration modes. Conditions: 1.0×10^{-6} mol L^{-1} BSA; slit width 5.0 nm; temperature 25 °C

synchronous fluorescence of BSA also help investigating the quenching mechanism of BSA fluorescence. When the interval ($\Delta=\lambda_{ex}$ - λ_{em}) between excitation and emission wavelengths is fixed, the fluorescence spectroscopy of tryptophan ($\Delta=60$ nm) and tyrosine ($\Delta=15$ nm) residues in BSA were obtained. Corresponding results show that tryptophan residues in BSA have a typical fluorescence peak around 338.0 nm (Fig. 6a) while tyrosine has a typical fluorescence peak around 299.0 nm (Fig. 6b). In traditional and calibration mode, the synchronous fluorescence for tryptophan and tyrosine both reduce successively with the increase of nanoAg and fluorescence quenching also happens (Fig. 6c and d). The synchronous fluorescence for tryptophan and tyrosine also show the consistent trends as that of BSA fluorescence. These also conclude that IFEs are the main reasons for the quenching of BSA synchronous fluorescence.

Conclusions

The work proves that it is feasible to calibrate the interference of IFEs in conventional cell using combined cells and outer filter effects. By altering absorbent concentrations in prepositive and side cells, the quenching of excitation and emission lights caused by the primary IFE and secondary IFE can be equally reduced by OFEs. The convenient correction method was directly used to evaluate the quenching mechanism of nanoAg to the fluorescence and synchronous fluorescence of BSA. Corresponding results make it clear that the IFEs caused by nanoAg, other than the static/dynamic fluorescent quenching, are the main reasons for the quenching of BSA fluorescence and synchronous fluorescence. The above strategy can also be applied to many different systems where the components have absorptions to the excitation and/or emission wavelengths of fluorescer.

Acknowledgements This work was supported by NSFC (20875055), Shanghai Tongji Gao Tingyao Environmental Science & Technology Development Fundation, Self-innovation foundation for graduate students in Shandong University (yzc09040), the Cultivation Fund of the Key Scientific and Technical Innovation Project, Ministry of Education of China (708058), SRF for ROCS, SEM and Excellent Young Scientists and Key Science-Technology Project in Shandong Province (2008GG10006012) are also acknowledged.

References

1. Marme N, Knemeyer JP, Sauer M, Wolfrum J (2003) Bioconjug Chem 14:1133–1139
2. Neuman D, Ostrowski AD, Mikhailovsky AA, Absalonson RO, Strouse GF, Ford PC (2008) J Am Chem Soc 130:168–175
3. Schneider G, Decher G, Nerambourg N, Praho R, Werts MH, Desce MB (2006) Nano Lett 6:530–536
4. Soares S, Mateus N, Freitas V (2007) J Agric Food Chem 55:6726–6735
5. Fanget B, Devos O, Draye M (2003) Anal Chem 75:2790–2795
6. Gu Q, Kenny JE (2009) Anal Chem 81:420–426
7. Mode VA, Sisson DH (1974) Anal Chem 46:200–203
8. Tohda K, Lu H, Umezawa Y, Gratzl M (2001) Anal Chem 73:2070–2077
9. Shang L, Dong SJ (2009) Anal Chem 81:1465–1470
10. Werner T, Klimant II, Wolfbeis OS (1994) J Fluoresc 4:41–44
11. Yang XF, Liu P, Wang L, Zhao M (2008) J Fluoresc 18:453–459
12. Leese RA, Wehry EL (1978) Anal Chem 50:1193–1197
13. Puchalski MM, Morra MJ, von Wandruszka R (1991) Fresenius J Anal Chem 340:341–344
14. Ramakrishna S, Rangarajan SK (1996) J Phys Chem 100:16365–16372
15. Domann R, Hardalupas Y, Jones AR (2002) Measurement. Sci Technol 13:280–291
16. MacDonalda BC, Lvinb SJ, Pattersonc H (1997) Anal Chim Acta 338:155–162
17. Christmann DR, Crouch SR, Tlmnick A (1981) Anal Chem 53:276–280
18. Chrlstmann DR, Crouch SR, Tlmnick A (1981) Anal Chem 53:2040–2044
19. Chi ZX, Liu RT, Zhao LZ, Qin PF, Pan XR, Sun F, Hao XP (2009) Spectrochim Acta A 72:577–581
20. Liu RT, Sun F, Zhang LJ, Zong WS, Zhao XC, Wang L, Hao XP (2009) Sci Total Environ 407:4184–4188
21. Zhang YZ, Chen XX, Dai J, Zhang XP, Liu YX, Liu Y (2008) Luminescence 23:150–156
22. Zhang YZ, Zhou B, Liu YX, Zhou CX, Ding XL, Liu Y (2008) J Fluoresc 18:109–118
23. Zhao LZ, Liu RT, Zhao XC, Yang BJ, Gao CZ, Hao XP, Wu YL (2009) Sci Total Environ 407:5019–5023
24. Bakr OM, Amendola V, Aikens CM, Wenseleers W, Li R, Dal LN, Schatz GC, Stellacci F (2009) Angew Chem Int Ed 48:5921–5926
25. Frederix F, Friedt JM, Choi KH, Laureyn W, Campitelli A, Mondelaers D, Maes G, Borghs G (2003) Anal Chem 75:6894–6900